Stem Cell Reports, Volume *6*

Supplemental Information

An *EWS-FLI1*-Induced Osteosarcoma Model Unveiled a Crucial Role of Impaired Osteogenic Differentiation on Osteosarcoma Development

Shingo Komura, Katsunori Semi, Fumiaki Itakura, Hirofumi Shibata, Takatoshi Ohno, Akitsu Hotta, Knut Woltjen, Takuya Yamamoto, Haruhiko Akiyama, and Yasuhiro Yamada

Figure S1

A

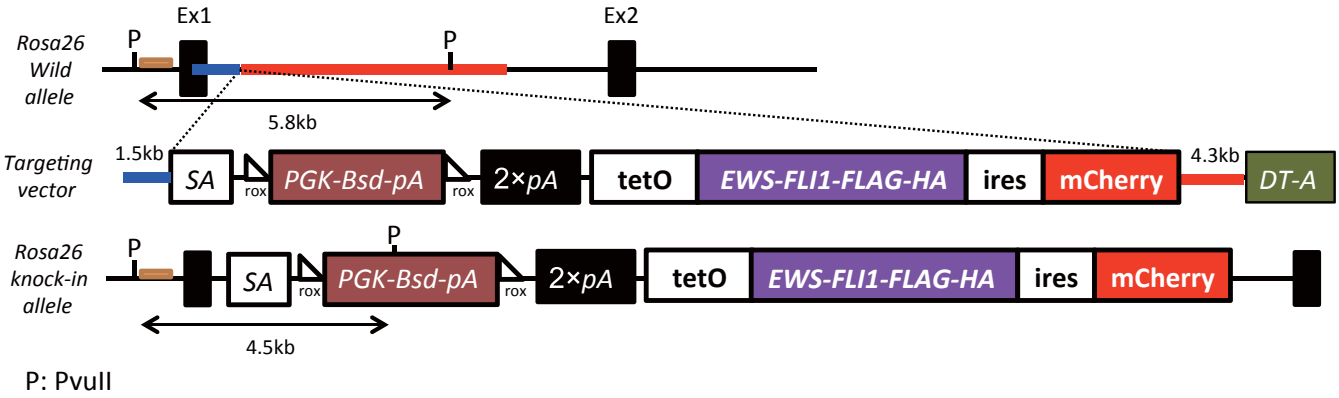

B

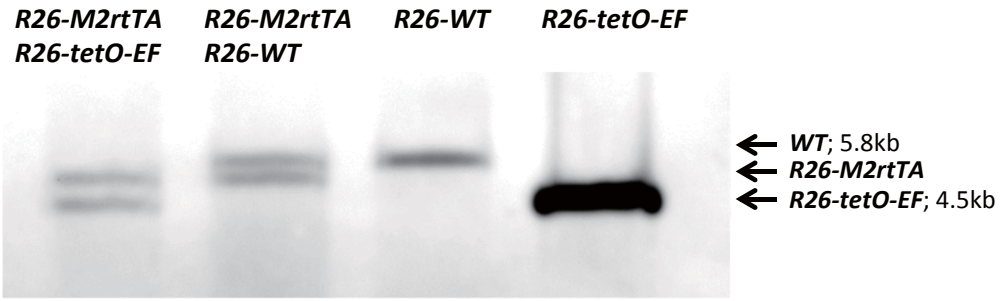

C

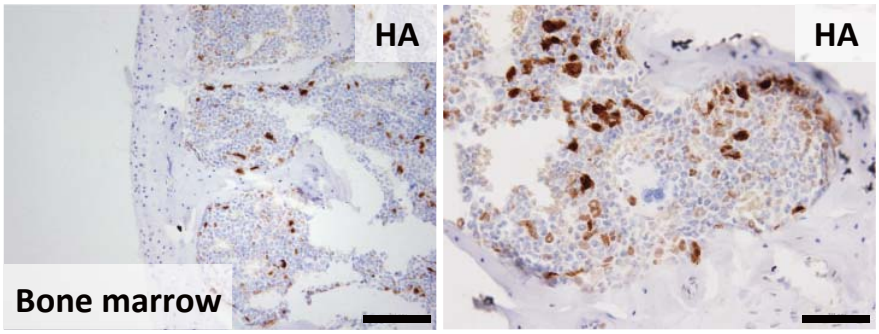

D

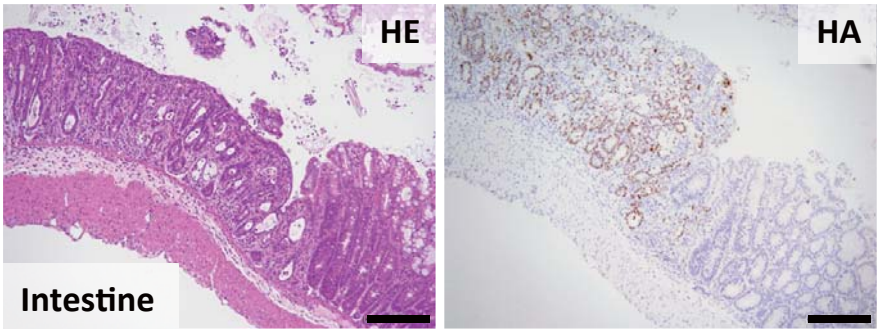

Figure S2

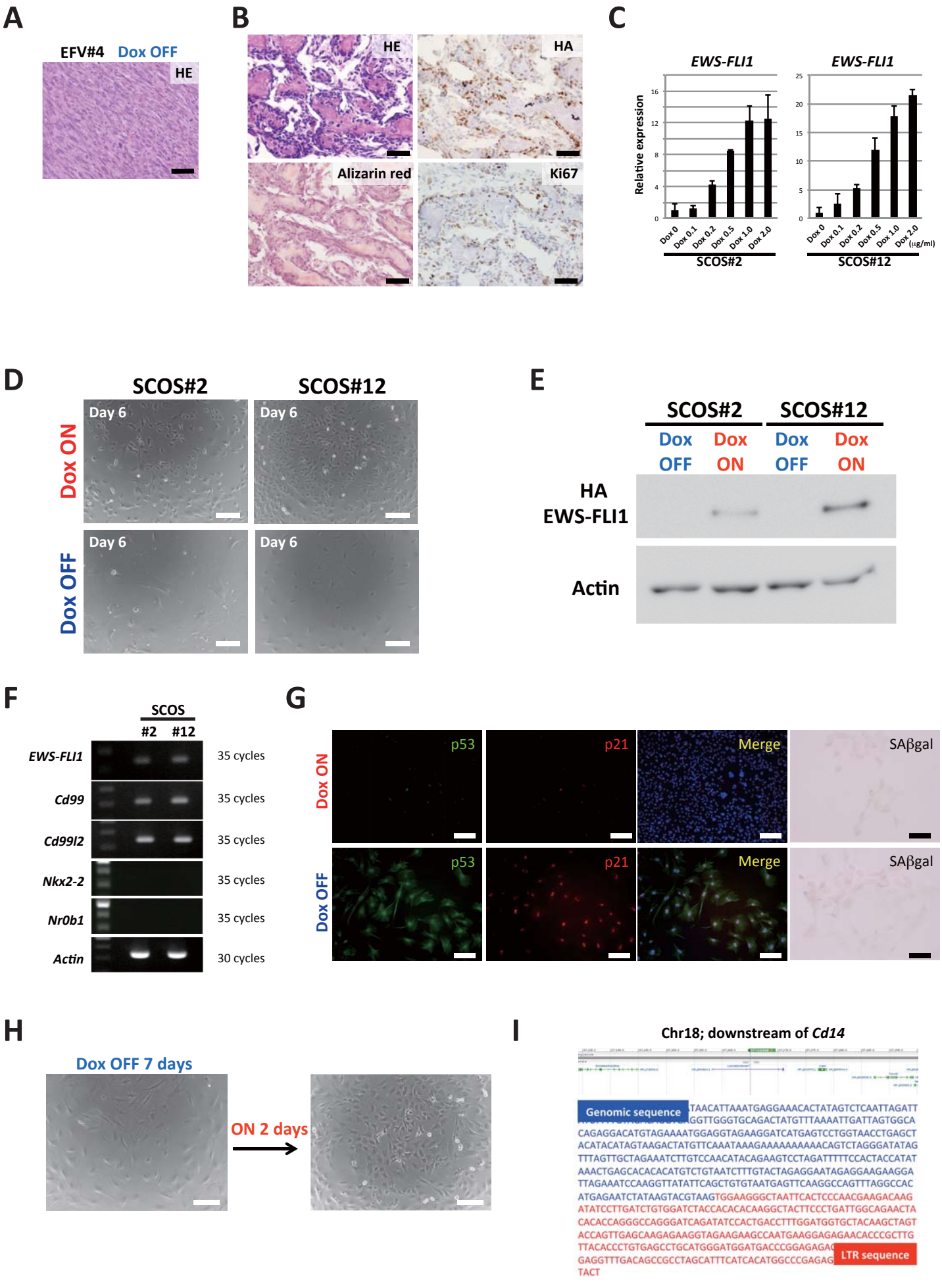
A
EFV#4 Dox OFF
HE
B
HE
HA
Alizarin red
Ki67
C
EWS-FLI1
EWS-FLI1
Relative expression
Dox 0
Dox 0.1
Dox 0.2
Dox 0.5
Dox 1.0
Dox 2.0
(μg/ml)
SCOS#2
SCOS#12
D
SCOS#2
SCOS#12
Dox ON
Dox OFF
Day 6
E
SCOS#2
SCOS#12
Dox OFF
Dox ON
HA
EWS-FLI1
Actin
F
SCOS
#2
#12
EWS-FLI1
Cd99
Cd99l2
Nkx2-2
Nr0b1
Actin
35 cycles
30 cycles
G
Dox ON
Dox OFF
p53
p21
Merge
SAβgal
H
Dox OFF 7 days
ON 2 days
I
Chr18; downstream of Cd14
Genomic sequence
LTR sequence

Figure S3

A

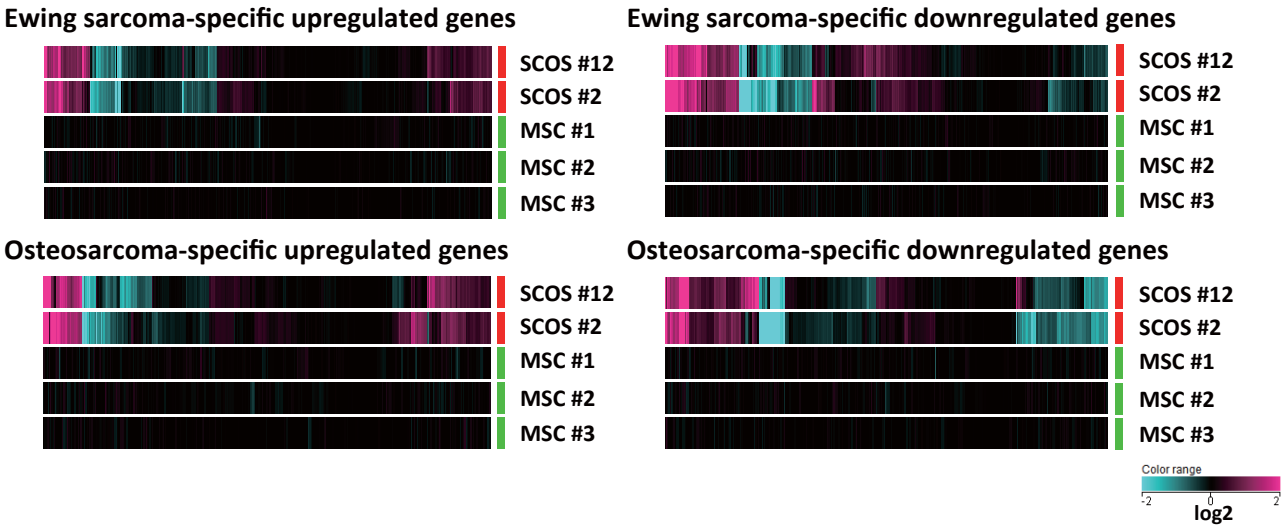

B

GO ACCESSION	GO Term	corrected p-value
GO:0005576	extracellular region	1.06E-21
GO:0044421	extracellular region part	2.16E-16
GO:0005615	extracellular space	9.86E-08
GO:0031012	extracellular matrix	7.89E-07
GO:0006950	response to stress	2.18E-05
GO:0006955	immune response	3.68E-05

C

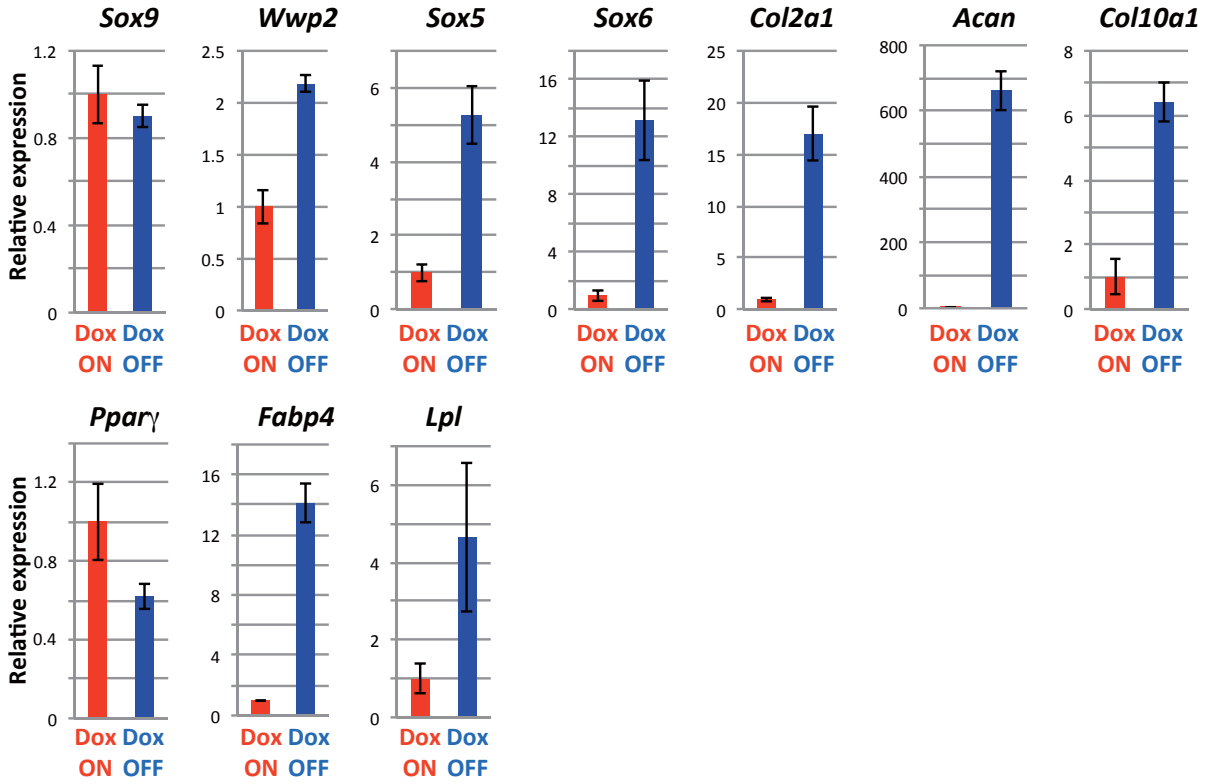

D

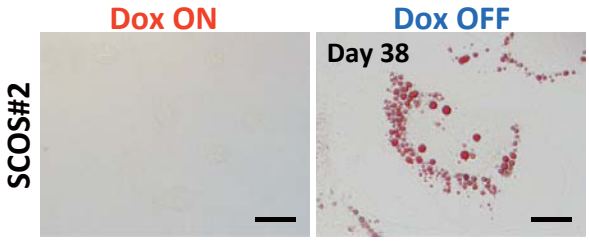

A

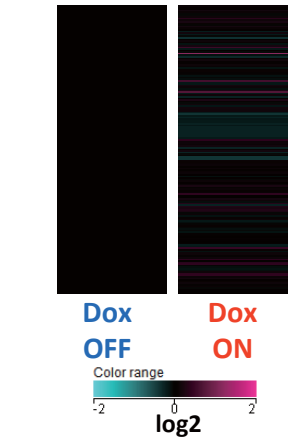

B

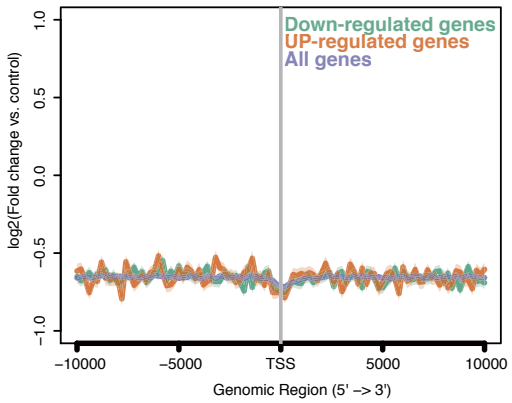

C

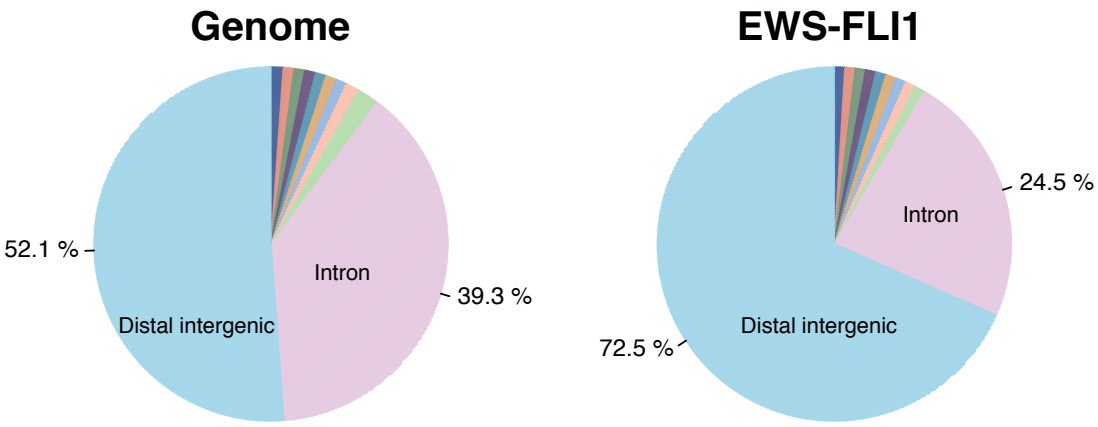

- Promoter (<=1000 bp): 1.1 %
- Promoter (1000–2000 bp): 0.8 %
- Promoter (2000–3000 bp): 0.7 %
- Downstream (<=1000 bp): 1.0 %
- Downstream (1000–2000 bp): 0.8 %
- Downstream (2000–3000 bp): 0.7 %
- 5'UTR: 0.3 %
- 3'UTR: 1.3 %
- Coding exon: 2.0 %
- Intron: 39.3 %
- Distal intergenic: 52.1 %

- Promoter (<=1000 bp): 0.2 %
- Promoter (1000–2000 bp): 0.4 %
- Promoter (2000–3000 bp): 0.5 %
- Downstream (<=1000 bp): 0.3 %
- Downstream (1000–2000 bp): 0.3 %
- Downstream (2000–3000 bp): 0.4 %
- 5'UTR: 0.1 %
- 3'UTR: 0.2 %
- Coding exon: 0.5 %
- Intron: 24.5 %
- Distal intergenic: 72.5 %

D

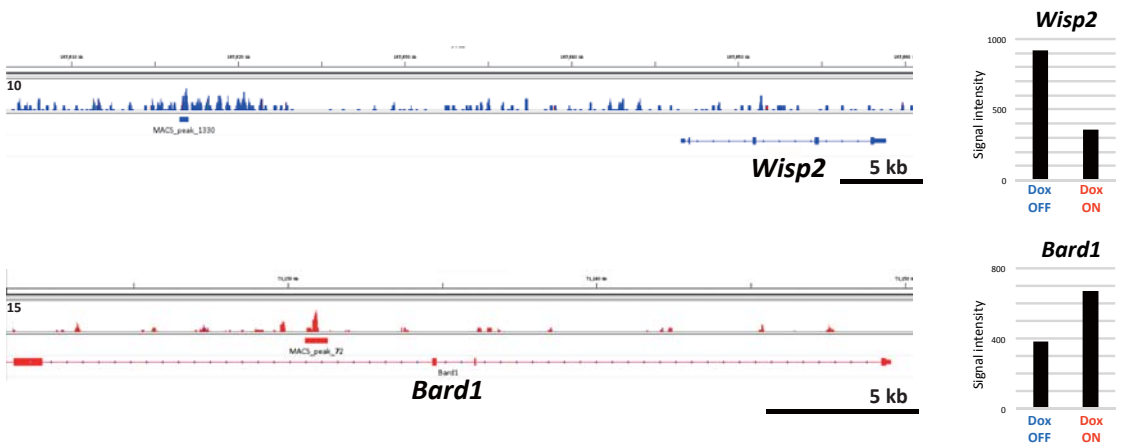

Figure S5

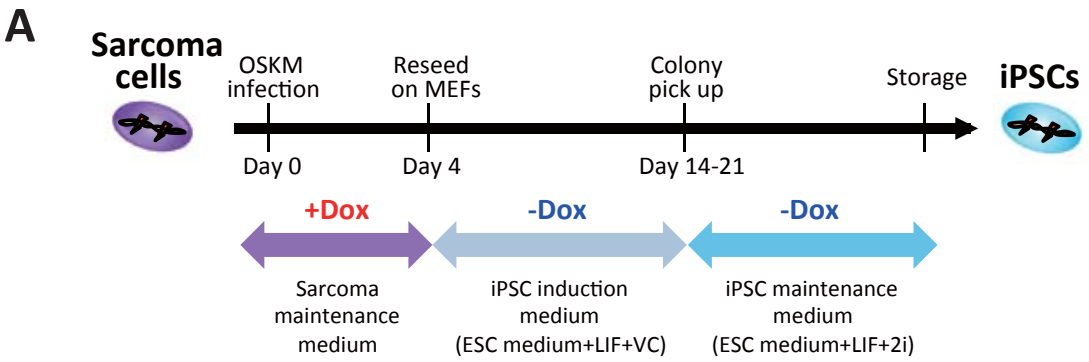
A
Sarcoma cells
OSKM infection
Reseed on MEFs
Colony pick up
Storage
iPSCs
Day 0
Day 4
Day 14-21
+Dox
-Dox
-Dox
Sarcoma maintenance medium
iPSC induction medium (ESC medium+LIF+VC)
iPSC maintenance medium (ESC medium+LIF+2i)

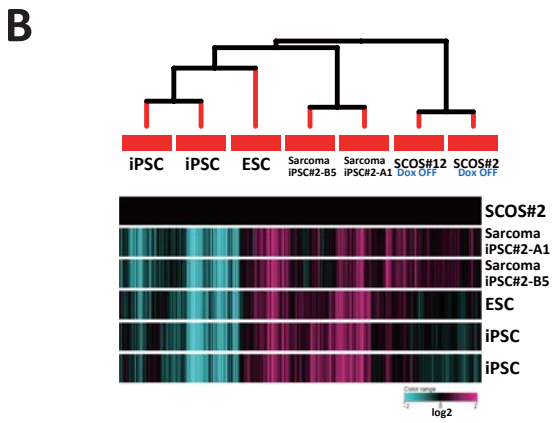
B
iPSC
iPSC
ESC
Sarcoma iPSC#2-B5
Sarcoma iPSC#2-A1
SCOS#12 Dox OFF
SCOS#2 Dox OFF
SCOS#2
Sarcoma iPSC#2-A1
Sarcoma iPSC#2-B5
ESC
iPSC
iPSC
log2

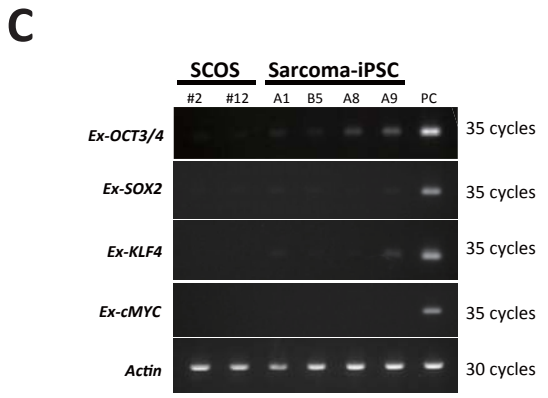
C
SCOS
Sarcoma-iPSC
#2
#12
A1
B5
A8
A9
PC
Ex-OCT3/4
Ex-SOX2
Ex-KLF4
Ex-cMYC
Actin
35 cycles
35 cycles
35 cycles
35 cycles
30 cycles

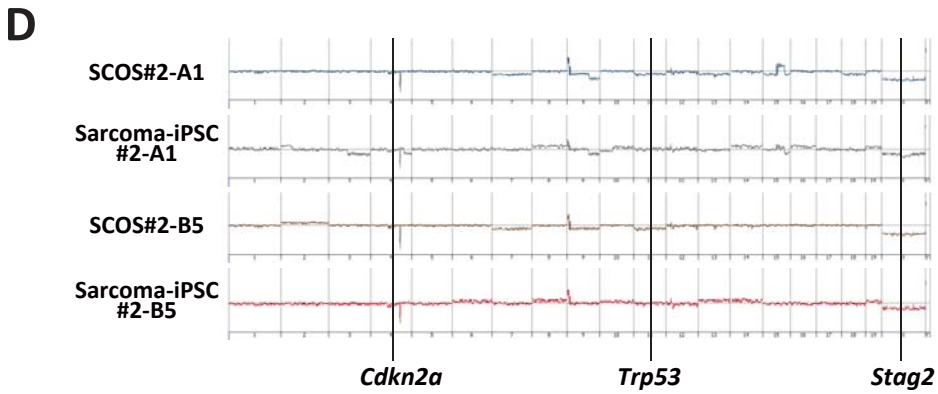
D
SCOS#2-A1
Sarcoma-iPSC #2-A1
SCOS#2-B5
Sarcoma-iPSC #2-B5
Cdkn2a
Trp53
Stag2

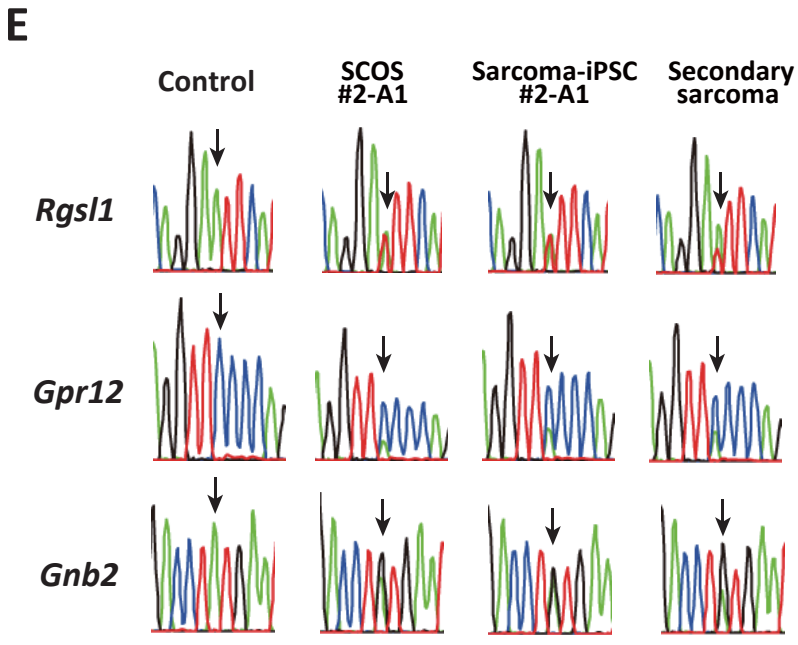
E
Control
SCOS #2-A1
Sarcoma-iPSC #2-A1
Secondary sarcoma
Rgsl1
Gpr12
Gnb2

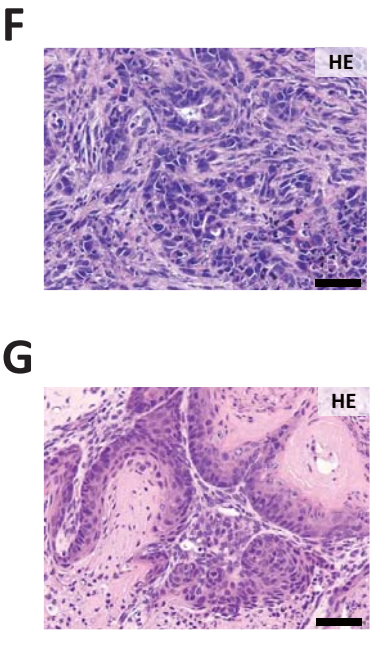
F
HE
G
HE

Table S1. Chimerism of examined mice

	Chimerism		
Genotype	Low (<30%)	Middle (30–60%)	High (>60%)
Rosa/Rosa	6	3	0
Rosa/Col	0	4	10
Total	6	7	10

Table S2. Candiate sites for unique missense mutation to *EWS-FLI1*-induced sarcoma model

Chr.	position (mm10)	REF	ALT	Gene symbol
chr1	26687331	A	G	4931408C20Rik
chr1	36419760	C	G	Fer1l5
chr1	78665011	G	A	Utp14b
chr1	85257408	C	T	C130026I21Rik
chr1	88055581	A	G	Ugt1a10
chr1	88055613	G	A	Ugt1a10
chr1	88056307	A	G	Ugt1a10
chr1	88256544	G	A	Mroh2a
chr1	153822346	A	T	Rgsl1
chr1	166146689	G	C	Gpa33
chr1	174836790	T	A	Grem2
chr2	37790432	C	G	Crb2
chr2	65098194	G	T	Cobll1
chr3	15548853	G	T	Sirpb1b
chr3	15548938	T	C	Sirpb1b
chr3	55783786	C	T	Mab21l1
chr3	108467915	G	A	5330417C22Rik
chr3	122936000	G	A	Usp53
chr4	40167087	C	T	Aco1
chr4	49792844	T	G	Grin3a
chr4	88571364	T	G	Ifna14
chr4	88816602	C	G	Ifna7
chr4	88835585	C	G	Ifna5
chr4	88835765	G	C	Ifna5
chr4	112835029	C	T	Skint6
chr4	112835089	T	A	Skint6
chr4	112872460	T	G	Skint6
chr4	112883687	C	A	Skint6
chr4	112894857	T	C	Skint6
chr4	113236373	G	T	Skint6
chr4	113238077	T	C	Skint6
chr4	113597739	C	A	Skint5
chr4	113691069	C	G	Skint5
chr4	113731063	T	A	Skint5
chr4	113827869	T	C	Skint5
chr4	113870717	C	T	Skint5
chr4	113923340	T	A	Skint5
chr4	113931810	C	G	Skint5
chr4	115762250	T	C	Efcab14
chr4	118917362	T	C	Olfr1329
chr4	134082593	C	T	Aim1l
chr4	147390321	A	G	Gm13145
chr4	156350965	T	C	Gm20782
chr5	87694785	C	T	Csn2
chr5	104065104	G	A	Nudt9
chr5	137529034	A	G	Gnb2
chr5	138240988	G	A	Nxpe5
chr5	146583613	C	A	Gpr12
chr6	97184820	T	A	Uba3
chr6	128357780	G	A	Rhno1
chr6	128357786	G	A	Rhno1
chr6	128357832	A	G	Rhno1
chr6	128357852	G	A	Rhno1
chr7	43225856	A	G	EU599041
chr7	48552900	G	T	Mrgprb2
chr7	97501779	T	A	Ints4
chr7	106677718	T	A	Olfr693
chr7	138836628	G	A	Mapk1ip1
chr7	140345816	G	T	Olfr60
chr8	17534910	C	T	Csmd1
chr8	36584125	T	C	Dlc1
chr8	110883353	C	T	Fuk
chr9	48450414	G	A	Gm5616
chr9	48450432	C	T	Gm5616
chr9	108955787	C	A	Col7a1
chr10	86905643	C	G	Stab2
chr11	58625248	G	A	Olfr323
chr11	58625303	C	G	Olfr323
chr11	58625761	G	A	Olfr323
chr11	58625792	T	G	Olfr323
chr11	58625905	A	C	Olfr323
chr11	58683931	G	T	Olfr320
chr11	58684256	G	A	Olfr320
chr11	58684462	C	T	Olfr320

chr11	58684714	G	A	Olfr320
chr11	58684721	T	C	Olfr320
chr11	58701957	A	C	Olfr319
chr11	58702326	C	T	Olfr319
chr11	58702395	C	A	Olfr319
chr11	58732373	T	G	Olfr317
chr11	58732648	T	C	Olfr317
chr11	58757966	G	A	Olfr316
chr11	58758068	C	T	Olfr316
chr11	58758104	A	G	Olfr316
chr11	58786946	A	G	Olfr314
chr11	116769067	G	T	St6galnac1
chr12	64473027	T	G	Fscb
chr12	76329274	T	C	Akap5
chr12	101418121	C	A	Catsperb
chr12	103693807	G	T	Serpina1f
chr12	104134219	G	C	Serpina3b
chr12	104340975	A	G	Serpina3k
chr12	113625541	T	C	Ighv5-6
chr12	113625945	C	A	Ighv5-6
chr12	113655233	G	C	Ighv5-8
chr12	113702423	T	A	Ighv5-12
chr12	113796269	A	T″	Ighv2-6-8
chr12	113796269	A	T″	Ighv2-6-8
chr12	113796269	A	T″	Ighv2-6-8
chr12	113796269	A	T″	Ighv2-6-8
chr12	113859405	T	G	Ighv5-17
chr12	113932083	C	T	Ighv14-1
chr12	113932196	G	A	Ighv14-1
chr12	113994755	G	T	Ighv14-2
chr12	114094228	G	A	Ighv9-1
chr12	114094229	C	T	Ighv9-1
chr12	114153426	A	T	Ighv7-3
chr12	114176681	G	A	Ighv14-4
chr12	114176691	G	A	Ighv14-4
chr12	114406948	G	T	Ighv6-4
chr12	114851275	A	T	Ighv1-34
chr12	114851307	C	T	Ighv1-34
chr12	114851322	T	A	Ighv1-34
chr12	114914615	C	T	Ighv1-39
chr12	114914857	A	T	Ighv1-39
chr12	115495818	T	G	Ighv1-63
chr12	115495858	C	T	Ighv1-63
chr12	115834373	A	G	Ighv1-75
chr12	115834392	C	G	Ighv1-75
chr12	115868845	T	G	Ighv1-78
chr13	61539620	C	T	Ctsm
chr13	61568124	C	T	Cts3
chr13	66431401	G	A	2410141K09Rik
chr13	66431419	C	T	2410141K09Rik
chr13	66431466	C	A	2410141K09Rik
chr13	66432161	G	T	2410141K09Rik
chr13	67256963	A	C	Zfp458
chr13	67256967	T	C	Zfp458
chr13	67256982	T	C	Zfp458
chr14	113315351	G	A	Tpm3-rs7
chr14	123954597	G	A	Itgbl1
chr15	73524148	G	A	Dennd3
chr15	98950656	C	G	Tuba1a
chr16	34666699	C	G	Ropn1
chr17	23311138	C	A	Vmn2r114
chr17	23311142	C	G	Vmn2r114
chr17	23346388	T	A	Vmn2r115
chr17	43064973	A	T	Tnfrsf21
chr18	12402904	A	T	Lama3
chr18	60269984	G	T	Gm4841
chr18	60270026	C	A	Gm4841
chr18	60270033	A	T	Gm4841
chr18	60270097	C	T	Gm4841
chr19	13410580	T	G	Olfr1469
chr19	37916431	C	T	Myof
chrX	7163391	C	A	Clcn5
chrX	21083065	A	T	Zfp300

Table S3. Overlapping mutations in murine *EWS–FLI1* sarcoma model and human sarcomas (Ewing sarcomas/PNETs and osteosarcomas)

Unique missense mutations in *EWS–FLI1*–induced sarcoma model		**Human Ewings sarcoma–peripheral primitive neuroectodermal tumour**		**Human osteosarcoma**	
Mouse gene symbol	Human gene symbol	Mutated samples (frequency) N=342	Detailed information	Mutated samples (frequency) N=58	Detailed information
Csmd1	CSMD1 (ENST00000537824)	15 (4.4%)	506 c.1518G>A p.S506S COSM1456746 1 Substitution – coding silent 1168 c.3502C>T p.R1168C COSM5030424 1 Substitution – Missense 1312 c.3934C>G p.P1312A COSM5030038 1 Substitution – Missense 1455 c.4365G>T p.L1455L COSM4588054 1 Substitution – coding silent 1533 c.4599C>T p.S1533S COSM1099201 1 Substitution – coding silent 1754 c.5260G>A p.G1754S COSM5029552 1 Substitution – Missense 1877 c.5631A>G p.V1877V COSM4588044 1 Substitution – coding silent 2138 c.6412C>T p.P2138S COSM4588042 1 Substitution – Missense 2220 c.6660A>T p.T2220T COSM4588040 1 Substitution – coding silent 2224 c.6672G>A p.T2224T COSM2789183 1 Substitution – coding silent 2340 c.7020T>A p.N2340K COSM5029445 1 Substitution – Missense 2760 c.8278G>A p.V2760M COSM4588034 1 Substitution – Missense 2807 c.8419C>T p.R2807C COSM274673 1 Substitution – Missense 2879 c.8635G>A p.A2879T COSM1623896 1 Substitution – Missense 2894 c.8682C>T p.N2894N COSM237253 1 Substitution – coding silent 2903 c.8709T>G p.S2903R COSM5030558 1 Substitution – Missense	4 (6.9%)	62 c.186C>T p.I62I COSM5023630 1 Substitution – coding silent 524 c.1570A>G p.K524E COSM5021556 1 Substitution – Missense 1774 c.5320C>A p.Q1774K COSM5024049 1 Substitution – Missense ? c.2593+3G>C p.? COSM5024485 1 Unknown
Col7a1	COL7A1	9 (2.6%)	327 c.979G>T p.A327S COSM4584435 1 Substitution – Missense 469 c.1405T>C p.Y469H COSM4584434 1 Substitution – Missense 593 c.1777C>T p.R593W COSM4584433 1 Substitution – Missense 1053 c.3159G>A p.A1053A COSM4584432 1 Substitution – coding silent 1156 c.3468C>T p.H1156H COSM4584431 1 Substitution – coding silent 1225 c.3673G>C p.A1225P COSM4584430 1 Substitution – Missense 1523 c.4567C>A p.P1523T COSM5030007 1 Substitution – Missense 2177 c.6527_6528insC p.G2177Tfs*113 COSM4584429 1 Insertion – Frameshift 2859 c.8575T>G p.S2859A COSM4584428 1 Substitution – Missense	N.D.	
Grin3a	GRIN3A	5 (1.5%)	493 c.1478A>T p.Y493F COSM3167357 1 Substitution – Missense 634 c.1902C>T p.I634I COSM4588303 1 Substitution – coding silent 708 c.2123G>A p.R708Q COSM3167342 1 Substitution – Missense 975 c.2925C>T p.T975T COSM5030015 1 Substitution – coding silent 1085 c.3254A>T p.Q1085L COSM4588302 1 Substitution – Missense	3 (5.2%)	554 c.1660T>C p.L554L COSM3982644 1 Substitution – coding silent 594 c.1781A>T p.D594V COSM1732353 1 Substitution – Missense 607 c.1821A>C p.A607A COSM3982643 1 Substitution – coding silent 1065 c.3194C>T p.A1065V COSM5023025 1 Substitution – Missense
Dennd3	DENND3	3 (0.9%)	449 c.1346C>T p.P449L COSM604520 1 Substitution – Missense 542 c.1626C>T p.S542S COSM4587797 1 Substitution – coding silent 974 c.2922C>A p.H974Q COSM4587798 1 Substitution – Missense 975 c.2923A>G p.S975G COSM4587799 1 Substitution – Missense	1 (1.7%)	363 c.1087C>T p.L363L COSM5021567 1 Substitution – coding silent
Dlc1	DLC1	3 (0.9%)	617 c.1850G>A p.R617Q COSM1096059 1 Substitution – Missense 651 c.1951T>C p.F651L COSM4587773 1 Substitution – Missense 1055 c.3163A>G p.S1055G COSM1250143 1 Substitution – Missense	N.D.	
Lama3	LAMA3	3 (0.9%)	1556 c.4668G>A p.P1556P COSM4580342 1 Substitution – coding silent 2672 c.8016C>T p.D2672D COSM2807632 1 Substitution – coding silent ? c.5112+1G>A p.? COSM4580344 1 Unknown	N.D.	
Myof	MYOF	3 (0.9%)	366 c.1096C>T p.R366* COSM4573900 1 Substitution – Nonsense 662 c.1984G>A p.A662T COSM4573897 1 Substitution – Missense 714 c.2142C>T p.N714N COSM3397310 1 Substitution – coding silent	N.D.	
Ugt1a10	UGT1A10	2 (0.6%)	50 c.150C>T p.L50L COSM3050195 1 Substitution – coding silent 374 c.1122T>C p.G374G COSM4583326 1 Substitution – coding silent	N.D.	
Crb2	CRB2	2 (0.6%)	93 c.277C>T p.R93C COSM4588458 1 Substitution – Missense 104 c.310C>T p.R104C COSM4588460 1 Substitution – Missense	N.D.	
Stab2	STAB2	2 (0.6%)	1041 c.3123C>T p.D1041D COSM4574950 1 Substitution – coding silent 1968 c.5903C>A p.A1968D COSM4574951 1 Substitution – Missense 2374 c.7121G>A p.R2374Q COSM4574953 1 Substitution – Missense	N.D.	
St6galnac1	ST6GALNAC1	2 (0.6%)	277 c.831G>A p.T277T COSM4580166 1 Substitution – coding silent 387 c.1159G>A p.D387N COSM4580165 1 Substitution – Missense	N.D.	
5330417C22Rik	KIAA1324	2 (0.6%)	351 c.1052T>C p.M351T COSM4576078 1 Substitution – Missense 898 c.2690_2691delAG p.R898fs*56 COSM4576079 1 Deletion – Frameshift	N.D.	
Aco1	ACO1	1 (0.3%)	876 c.2628C>T p.N876N COSM4588759 1 Substitution – coding silent	1 (1.7%)	630 c.1889C>T p.S630L COSM5024313 1 Substitution – Missense
Akap5	AKAP5	1 (0.3%)	350 c.1050T>C p.F350F COSM4577961 1 Substitution – coding silent	1 (1.7%)	184 c.550G>A p.E184K COSM1300753 1 Substitution – Missense
Clcn5	CLCN5	1 (0.3%)	460 c.1380T>A p.A460A COSM4589464 1 Substitution – coding silent	1 (1.7%)	390 c.1169A>C p.N390T COSM5023942 1 Substitution – Missense
Tnfrsf21	TNFRSF21	1 (0.3%)	48 c.144G>A p.S48S COSM1079994 1 Substitution – coding silent	1 (1.7%)	483 c.1447C>T p.R483C COSM5024184 1 Substitution – Missense
Zfp458	ZNF43	1 (0.3%)	717 c.2150G>A p.R717Q COSM4580861 1 Substitution – Missense	1 (1.7%)	737 c.2209G>A p.E737K COSM5022020 1 Substitution – Missense
Cobll1	COBLL1	1 (0.3%)	973 c.2917G>A p.D973N COSM5030279 1 Substitution – Missense	N.D.	
Mab21l1	MAB21L1	1 (0.3%)	244 c.731G>A p.G244E COSM4575915 1 Substitution – Missense	N.D.	
Aim1l	AIM1L	1 (0.3%)	558 c.1674G>T p.E558D COSM4577167 1 Substitution – Missense	N.D.	
Gnb2	GNB2	1 (0.3%)	291 c.871_880del10 p.D291fs*7 COSM3080668 1 Deletion – Frameshift	N.D.	
Catsperb	CATSPERB	1 (0.3%)	41 c.122C>T p.P41L COSM4578062 1 Substitution – Missense	N.D.	
Itgbl1	ITGBL1	1 (0.3%)	365 c.1093G>T p.D365Y COSM4575812 1 Substitution – Missense	N.D.	
Ifna5 Ifna7 Ifna14	IFNA4	1 (0.3%)	60 c.179G>C p.G60A COSM4588738 1 Substitution – Missense	N.D.	
Mrgprb2	MRGPRX1	1 (0.3%)	245 c.733G>T p.D245Y COSM4574247 1 Substitution – Missense	N.D.	
Olfr314	OR2T8	1 (0.3%)	56 c.167C>T p.P56L COSM2232658 1 Substitution – Missense	N.D.	
Zfp300	ZNF567	1 (0.3%)	409 c.1225_1233delGAGAAA... p.E409_T411delEKT COSM5030662 1 Deletion – In frame	N.D.	
Gpa33	GPA33	N.D.		1 (1.7%)	138 c.413T>C p.L138P COSM5023795 1 Substitution – Missense
Fscb	FSCB	N.D.		1 (1.7%)	805 c.2414C>T p.A805V COSM5023103 1 Substitution – Missense
Olfr323	OR11L1	N.D.		1 (1.7%)	217 c.650C>G p.P217R COSM5023988 1 Substitution – Missense

N.D.; not detected

Table S4. Primer sequence

	Genes	Forward (5' ⇒ 3')	Reverse (5' ⇒ 3')	
qRT-PCR	*EWS-FLI*	CAATATAGCCAACAGAGCAGCAG	CTCCAAGGGGAGGACTTTTG	
	Nanog	TGCTTACAAGGGTCTGCTACTG	TAGAAGAATCAGGGCTGCCTTG	
	Oct3/4 (endogenous)	TCCCATGCATTCAAACTGAG	CCACCCCTGTTGTGCTTTTA	(Ohnishi, Semi et al. 2014)
	Runx2	ACAGTCCCAACTTCCTGTGC	TTCTCATCATTCCCGGCCATG	
	Sp7	TTCTCTCCATCTGCCTGACTCC	GCTAGAGCCGCCAAATTTGC	
	Col1a1	TGGCGGTTATGACTTCAGCTTCCT	GGTCACGAACCACGTTAGCATCAT	
	Pth1r	CCAACTACAGCGAGTGCCTC	GGTGAGGGAGGCAAGAGACA	
	Bglap	AGTGTGAGCTTAACCCTGCTTG	ATGCGTTTGTAGGCGGTCTTC	
	Dmp1	TGATTTGGCTGGGTCACCAC	TGTCCGTGTGGTCACTATTTGC	
	Sost	AGAACAACCAGACCATGAACCG	TGTACTCGGACACATCTTTGGC	
	Fgf23	CCACGGCAACATTTTTGGATCG	TGCGACAAGTAGACGTCATAGC	
	Mepe	ATGAAGATGCAGGCTGTGTCTG	AGATGCTGCCAAGTCCTTGTG	
	Sox9	GCAAGCTGGCAAAGTTGATCTG	ACGTCGAAGGTCTCAATGTTGG	
	Wwp2	AAGTGGAGCGGAGTTAGGC	AAGCTGGGACTTCTCAAAAGG	
	Sox5	CTTTCCCGACATGCACAATTCC	TACTTCTCCAGGTGCTGTTTGC	
	Sox6	ATGGCAAGAAGCTCCGGATTG	AACACCTGTTCCTGTGGTGATG	
	Col2a1	CCAAACACTTTCCAACCGCAGTCA	AGTCTGCCCAGTTCAGGTCTCTTA	
	Acan	TTCACTGTAACCCGTGGACT	TGGTCCTGTCTTCTTTCAGC	
	Col10a1	ATAGGCAGCAGCATTACGAC	TAGGCGTGCCGTTCTTATAC	
	Pparg	GCTGTGAAGTTCAATGCACTGG	TGCAGCAGGTTGTCTTGGATG	
	Fabp4	ATGAAATCACCGCAGACGACAG	ATTGTGGTCGACTTTCCATCCC	
	Lpl	AGCCAAGAGAAGCAGCAAGATG	AAATCTCGAAGGCCTGGTTGTG	
	Actb	GCCAACCGTGAAAAGATGAC	TCCGGAGTCCATCACAATG	
RT-PCR	*Cd99*	AAGGCCACACGGAGACTCAG	TGATAGGCCACGAAGCTCGA	
	Cd99l2	TCAGCACCACGACTAGGAGG	GTATCCCCCACCTTCCACGA	
	Nkx2-2	ACCAACACAAAGACGGGGTT	GTCATTGTCCGGTGACTCGT	
	Nr0b1	ATGGAGATCCCGGAGACCAA	GGATCTGCTGGGTTCTCCAC	
	Ex-hOCT3/4	GCTCTCCCATGCATTCAAACTGA	CTTACGCGAAATACGGGCAGACA	
	Ex-hSOX2	TTCACATGTCCCAGCACTACCAGA	GACATGGCCTGCCCGGTTATTATT	
	Ex-hKLF4	CCACCTCGCCTTACACATGAAGA	GACATGGCCTGCCCGGTTATTATT	
	Ex-h-cMYC	ATACATCCTGTCCGTCCAAGCAGA	GACATGGCCTGCCCGGTTATTATT	
	Actb	GCTACAGCTTCACCACCACA	CTTCTGCATCCTGTCAGCAA	
Bisulfite genomic sequence	*Nanog* promoter	GATTTTGTAGGTGGGATTAATTGTGAATTT	ACCAAAAAAAACCCACACTCATATCAATATA	(Takahashi and Yamanaka 2006)
	Oct3/4 distal enhancer	GGTTTTAGAGGTTGGTTTTGGG	CATCTCTCTAACCCTCTCCATAAATC	(Theunissen, Costa et al. 2011)

		5' ⇒ 3'	
Virus integration site detection	Asymmetric linker cassette LC1_adaptor	GACCCGGGAGATCTGAATTCAGTGGCACAG	
	Asymmetric linker cassette LC2_adaptor	CTGTGCCACTG	
	1st_PCR_AP1_F	GACCCGGGAGATCTGAATTC	
	1st_PCR_pSLIK1_R	GTCGAGAGAGCTCCTCTGGTTTC	(Varas, Stadtfeld et al. 2009)
	2nd_PCR_AP2_F	CCTATCCCCTGTGTGCCTTGGCAGTCTCAGGATCTGAATTCAGTGGCACAG	
	2nd_PCR_pSLIK2_R	CTTTCGCTTTCAAGTCCCTGTTCG	
	3rd_seq_LTR_R	CTCAAGGCAAGCTTTATTGAGGC	

Legends to Supplemental Figures

Figure S1; Related to Figure1. *Rosa-M2rtTA/Rosa::tetO-EWS-FLI1* system and phenotype caused by *EWS-FLI1* expression in mice.

A. Schematic representation of the *Rosa26* targeting allele. *tetO-EWS-FLI1-ires-mCherry* is inserted into intron 1 of the *Rosa26* locus. SA, splice acceptor; ires, internal ribosome entry site; pA, poly(A) sequence; DT-A, diphtheria toxin A.

B. Southern blot analysis of the Bsd resistant clone using a 5' external probe. Note that the obtained clone harbors both the *Rosa26-M2rtTA* allele and *Rosa26::tetO-EWS-FLI1* allele.

C. Anti-HA immunostaining of bone in *Rosa*::*M2rtTA/Col1a1*::*tetO-EWS-FLI1* mice. EWS-FLI1 positive cells are observed in the bone marrow after Dox treatment. Scale bars, 100 μm (left) and 50 μm (right).

D. EWS-FLI1 expressing cells exhibit dysplastic change in the intestine of *Rosa-M2rtTA/Col1a1*::*tetO-EWS-FLI1* mice. Scale bars, 200 μm.

Figure S2; Related to Figure2. Characterization of *EWS-FLI1*-dependent osteosarcoma cell lines SCOS#2 and SCOS#12.

A. EFV#4 developed spindle cell sarcomas in immunocompromised mice even in the absence of Dox. Scale bar, 50 μm.

B. *EWS-FLI1*-induced tumor (EFN#2) was negative for Alizarin red staining. Immunohistochemistry using HA and Ki67 antibody revealed that *EWS-FLI1*-induced tumor expresses EWS-FLI1 and has high proliferative activity. Scale bars, 50 μm.

C. qRT-PCR analysis shows that both SCOS#2 and SCOS#12 express *EWS-FLI1* mRNA in a Dox concentration-dependent manner (0.1-2.0 μg/ml). Data are presented as mean ± SD. The expression level of Dox 0 cells was set to 1.

D. Morphology of the *EWS-FLI1*-dependent sarcoma cell lines SCOS#2 and SCOS#12 (top). Both cell lines changed their morphology to large and flat cells 6 days after Dox withdrawal (bottom). Scale bars; 200μm.

E. The sarcoma cell lines express EWS-FLI1 protein in the presence of Dox. EWS-FLI1 protein was detected by western blotting using anti-HA antibody.

F. RT-PCR analysis shows that SCOS#2 and SCOS#12 express surface antigen *Cd99*, which is marker of human Ewing sarcoma, and its variant *Cd99l2*. However, *Nkx2-2* and *Nr0b1*, direct targets of *EWS-FLI1* in Ewing sarcoma, were undetectable, suggesting that SCOS#2 and SCOS#12 have

different properties from Ewing sarcoma.

G. Immunocytochemistry for p53 and p21. The withdrawal of Dox leads to the increased expression of p53 and p21 and to growth arrest. Senescence associated beta-galactosidase (SAβgal) activity was not observed. Scale bars, 200 μm (first three columns) and 50 μm (right column).

H. Re-administration of Dox gives proliferative potential to resting sarcoma cells, suggesting that the cell cycle arrest was induced in sarcoma cells by the withdrawal of *EWS-FLI1* expression. Scale bars; 200μm.

I. The lentivirus integration site was investigated by LM-PCR (Varas et al., 2009). The analysis identified the integration site downstream region of the *Cd14* gene.

Figure S3; Related to Figure3. Gene expression change in *EWS-FLI1*-dependent osteosarcoma cell lines

A. Expression of upregulated and downregulated genes in human Ewing sarcomas and human osteosarcomas in SCOS#2 and SCOS#12. Note that SCOSs exhibit a partial similarity with both human Ewing sarcomas and human osteosarcomas. Published microarray data of 8 human Ewing sarcomas (GSM213306, GSM213307, GSM213308, GSM213309, GSM213310, GSM510019, GSM510022 and GSM510025), 3 human MSCs (GSM906367, GSM906368 and GSM906369), 8 human osteosarcomas (GSM1349294, GSM1517387, GSM1727193, GSM1727195, GSM1727196, GSM1727197, GSM1893361 and GSM1893364) and 3 murine MSCs (GSM1180589, GSM1180590 and GSM1180591) were used (Feng et al., 2015; Grilli et al., 2015; Kawano et al., 2015; Lu et al., 2015; Mackintosh et al., 2012; Miyagawa et al., 2008; Ullah et al., 2014). For this analysis, we first extracted upregulated and downregulated genes in human Ewing sarcomas and human osteosarcomas when compared with human MSCs (two folds). Then, upregulated and downregulated genes specific to Ewing sarcoma or osteosarcoma were identified by comparing the two gene sets (two folds higher or lower in each sarcoma type), respectively. Gene symbols in a human microarray platform (GeneChip U133 Plus 2.0 Array) were converted to gene symbols in a mouse microarray platform (GeneChip Mouse Gene 1.0ST Array) and analyzed for gene expressions.

B. Gene ontology enrichment analysis showed that extracellular region and matrix-related genes are upregulated in Dox OFF (72 hrs after withdrawal) compared to Dox ON in SCOS#12. The upregulated genes were selected by a cutoff point at fold change >2.0 and p-value <1.0E-4. The top 4 enriched clusters are highlighted.

C. The increased expression of chondrogenic and adipogenic differentiation-related genes in sarcoma cells at 38 days after Dox withdrawal. mRNA expression levels were measured by qRT-PCR. Data

are presented as mean ± SD. The expression level of Dox ON cells was set to 1.

D. At 38 days after Dox withdrawal, sarcoma cells exhibited positive staining for Oil red O. Scale bars; 20μm.

Figure S4; Related to Figures 3. ChIP-seq analysis for EWS-FLI1 binding to SCOS#2.

A. Genes which possess EWS-FLI1 binding sites close to their TSS (±5 kb, 126 genes and 181 probe sets) were analyzed for their expression. No obvious difference in the expression levels was detected between Dox ON and OFF sarcomas.

B. EWS-FLI1-binding near the TSSs of upregulated/downregulated genes. No obvious enrichment was observed in either upregulated or downregulated genes.

C. The distribution of EWS-FLI1 binding sites. Right: regions of EWS-FLI1 binding to SCOS#2, Left: regions of the reference genome. EWS-FLI1 preferentially binds to the distal intergenic region of SCOS#2.

D. Representative genes (*Wisp2* and *Bard1*) dysregulated in SCOS#2. EWS-FLI1 binds at the distal intergenic region near *Wisp2* and at the intron of *Bard1*.

Figure S5; Related to Figures 4 and 5. Characterization of sarcoma-derived iPSCs and secondary sarcomas derived from these iPSCs.

A. Schematic illustration of the iPSC derivation protocol from *EWS-FLI1*-dependent osteosarcoma cells.

B. Hierarchical clustering analysis of *EWS-FLI1*-induced sarcoma, sarcoma-iPSCs and control ESCs/iPSCs (GSE45916) (Ohta et al., 2013). Comparison of global gene expressions by microarray analysis indicated that sarcoma-iPSCs have normal PSC-like gene expression patterns. Color range is shown using a log2 scale.

C. RT-PCR showed the silencing of exogenous *OCT3/4, SOX2, KLF4* and *cMYC* expression in established sarcoma-iPSC-like cells.

D. Array CGH analysis of parental sarcoma cells and the established iPSCs. Some chromosomal abnormalities are identical between sarcoma-derived iPSCs and the parental sarcoma cells. The locations of *Stag2*, *Trp53*, and *Cdkn2a*, which are common mutated genes in human Ewing sarcoma, are indicated. SCOS#2 was established from bone marrow stromal cells of male *Rosa26-M2rtTA* mouse. Genomic DNA from female C57BL/6 mice was used as reference for the CGH analysis.

E. Direct sequencing results of representative genetic mutations in sarcoma cells (SCOS#2), sarcoma-iPSCs and the secondary sarcoma, which were identified by exome analysis.

F. Secondary sarcomas derived from the sarcoma-iPSCs often contain the carcinoma component. Scale

bar, 50 μm.

G. Parakeratosis of squamous epithelium is detected in sarcoma iPSCs-derived teratomas, which implies the impairment of terminal differentiation. Scale bar, 50 μm.

Supplemental Experimental Procedures

Rosa26 targeting vector, ESC targeting and generation of chimeric mice

The *EWS-FLI1* type1 fusion gene was cloned from Ewing sarcoma cell line TC135 (Takigami et al., 2011). For the *Rosa-M2rtTA/Rosa*::*tetO-EWS-FLI1* system, the Red/ET BAC recombination system was used to introduce *TetOP-EWS-FLI1-FLAG-HA-ires-mCherry-pA* and the selection cassette (*SA-rox-PGK-EM7-BsdR-pA-rox-2pA*) into intron 1 of *Rosa26* BAC. The obtained vector was electropolated to KH2 ESCs, which had the *Rosa26-M2rtTA* allele (Beard et al., 2006). ESCs were cultured with ES media containing 15 μg/ml BlasticidinS (Bsd, Funakoshi). Bsd-resistant colonies were picked up and expanded. Correctly targeted ES clones were confirmed by Southern blotting. For the *Rosa-M2rtTA/Col1a1*::*tetO-EWS-FLI1* system, the *EWS-FLI1-FLAG-HA-ires-mCherry-pA* sequence was inserted into pBS31, which was electropolated into KH2 ESCs as described previously (Beard et al., 2006). In both systems, chimeric mice were obtained by blastocyst injection.

Lentivirus vector construction, lentivirus infection and cell culture

To construct the doxycycline inducible lentiviral vector, we modified pEN-TmiRC3 and pSLIK-Neo lentiviral vector plasmids obtained from Addgene. First, pEN-TmiRC3 was digested with SpeI and XhoI to ligate *EWS-FLI1-FLAG-HA* downstream of the tetOP-mCMV promoter. Subsequently, the *ires-NeoR* cassette was ligated at the 3' of HA tag, followed by the excision of the *UbiC-rtTA3-ires-NeoR* sequence from pSLIK-Neo. After LR recombination between pEN-TmiRC3 (*tetO-EWS-FLI1-ires-Neo*) and pSLIK (without *UbiC-rtTA3-ires-Neo*), we obtained the pSLIK-*TetO-EWS-FLI1-ires-Neo* vector.

Bone marrow stromal cells were obtained from *Rosa26-M2rtTA* mice (Beard et al., 2006) at 3-4 weeks of age as reported previously (Soleimani and Nadri, 2009). At 3-4 days after the harvesting of bone marrow cells, non-adherent cells (hematopoietic cells) were removed by changing the culture media, and the adherent cells were infected with lentivirus. The cells were then cultured with DMEM (Nacalai) containing 10% FBS (Gibco), penicillin, streptomycin, 200 μg/ml G418 (Nacalai) and 2 μg/ml Dox (Sigma) for 2 months, and *EWS-FLI1*-dependent immortalized cells were established. Osteosarcoma cell lines, SCOS#2 and SCOS#12, were maintained in the same medium.

Single cell cloning

Single cell sorting of SCOS#2 and SCOS#12 cells was performed by FACS (Aria II, BD) in 96-well culture plates. Each sorted cell was cultured and expanded with Dox- and G418-containing

medium.

Cell growth assay

Sarcoma cells and ESCs/iPSCs were plated into 12 well culture plates at a density of 5×10^4 cells/well and 1×10^5 cells/well, respectively. The experiment was performed in triplicate, and each sample was measured twice. The number of cells was measured by an automatic cell counter (TC10^{TM}, Bio-Rad).

Xenograft assay

A total of 3×10^6 *EWS-FLI1*-dependent immortalized cells, *EWS-FLI1*-dependent sarcoma cells or ESCs/iPSCs were transplanted to NOD/ShiJic-scid Jcl mice or BALB/cSLC-nu/nu mice purchased from CLEA Japan and Japan SLC, respectively. *EWS-FLI1*-dependent immortalized cells were inoculated into NOD/ShiJic-scid Jcl mice, which were sacrificed at 10 weeks after the transplantation. *EWS-FLI1*-dependent osteosarcoma cells were inoculated into the subcutaneous tissue of BALB/cSLC-nu/nu mice. The tumor size was measured with digital calipers every week, and tumor volume was calculated as follows: volume = width$^2\times$length$\div$2. ESCs/iPSCs were transplanted into BALB/cSLC-nu/nu mice, and teratomas were obtained after 3-4 weeks.

RT-PCR and real-time quantitative RT-PCR

RNA was extracted using RNeasy Plus Mini Kit (QIAGEN). Up to 1 μg RNA was used for the reverse transcription reaction into cDNA. RT-PCR and real-time quantitative PCR were performed using Go-Taq Green Master Mix and Go-Taq qPCR Master Mix (Promega), respectively. Transcript levels were normalized by β-actin. PCR primers are available in Table S4.

Western blot analysis

Cultured cells were harvested in 500 μl of RIPA lysis buffer, and protein concentration was measured. Proteins were denatured with 2×SDS in 95 ℃ for 5 min. A total of 20 μg denatured protein was applied to 10% SDS/PAGE gel and transferred to PVDF membrane (Amersham Hybond-P PVDF Membrane, GE HealthCare). Proteins were detected by immunoblotting with anti-HA (Cell Signaling, C29F4, #3724; dilution 1:600) and anti-β actin (Santa Cruz, C4, sc-47778; dilution 1:1000) antibodies. Pierce ECL plus Western Blotting Substrate (Thermo Scientific) was used for visualization, and LAS4000 (GE HealthCare) was used for detection.

Histological analysis and immunohistochemistry

All tissue and tumor samples were fixed with 4% paraformaldehyde overnight and embedded in paraffin. Sections were stained with hematoxylin and eosin using standard protocol. For immunohistochemistry, the antibodies used were anti-HA (Cell signaling, C29F4, #3724; dilution 1:200) and anti-Ki67 (Abcam, SP6, ab16667; dilution 1:150).

Immunocytochemistry

Cultured cells were washed with PBS and fixed with 2% paraformaldehyde for 10 min at room temperature. For immunocytochemistry, antibodies used were anti-p53 (Abcam, PAb240, ab26; dilution 1:200) and anti-p21 (Abcam, HUGO291, ab107099; dilution 1:500).

ALP staining

Cultured cells were washed with PBS, fixed and stained with ALP Staining Kit (Sigma) according to the manufacturer's protocol.

Senescence-associated β -gal staining

Cultured cells were washed with PBS, fixed and stained with Senescence β-galactosidase Staining Kit (#9860S, Cell Signaling) according to the manufacturer's protocol.

Alizarin red staining

Cultured cells were washed with PBS and fixed with 4% paraformaldehyde for 5 min at room temperature. Fixed cells were washed with de-ionized water several times and stained in Alizarin red staining solution for 5 min (Alizarin red (Sigma, A5533) 2%, pH4.2 adjusted with NH_4OH). Similarly, de-paraffinized sections were stained in Alizarin red staining solution for 5 min.

Oil red O staining

Cultured cells were washed with PBS and fixed with 4% paraformaldehyde for 10 min at room temperature. Fixed cells were washed with 60% iso-propanol for 1 min and stained in oil red staining solution for 10 min (Oil red O (Sigma, O0625) 0.18% with 60% iso-propanol).

Detection of lentivirus integration site

We explored lentivirus integration sites as previously described with slight modifications (Varas et al., 2009). Extracted genomic DNA from SCOS#2 was digested into 500-800 bp fragments with

an ultrasonicator (Covaris E210). The linker-cassette obtained from annealing LC1 and LC2 was attached to the digested genomic DNA fragments. Subsequently, the first PCR was performed with AP1_F and pSLIK1_R primer set, followed by a nested PCR with AP2_F and pSLIK2_R primer set. PCR products were cloned to the pCR4-TOPO vector (Invitrogen) by the TA cloning method, and DNA sequences of the inserted fragments were analyzed by 3500xL Genetic Analyzer (Applied Biosystems) with seq_LTR_R primer. The obtained sequences were explored in at the BLAST website (http://blast.ncbi.nlm.nih.gov/Blast.cgi).

Bisulfite genomic sequencing

Bisulfite treatment was performed using the EZ DNA Methylation-Gold Kit^{TM} (ZYMO RESEARCH) according to the manufacturer's protocol. The PCR primers used are shown in Supplemental information. Amplified products were cloned into the pCR4-TOPO vector (Invitrogen) and transformed into DH5α. Colonies were randomly selected and sequenced with M13 forward and reverse primers for each gene.

ChIP-seq analysis

ChIP (Formaldehyde-Assisted Isolation of Regulatory Elements) was performed as described previously (Arioka et al., 2012). Anti-HA antibody (Nacalai, HA124, 06340-54) was used for the ChIP-seq analysis. Sequencing libraries were generated using TruSeq ChIP Sample Prep Kit (Illumina), assessed on an Agilent Bioanalyzer and quantified with KAPA Library Quantification Kits (KAPA BIOSYSTEMS). The libraries were sequenced to generate single-end 100 bp reads using Illumina MiSeq. We analyzed ChIP-seq data by mapping the reads using Bowtie2. The sequencing reads were aligned to mouse genome build mm9. We used the MACS (Zhang et al., 2008) version 1.4.2 peak finding algorithm to identify regions of ChIP-seq enrichment over background with p value 1×10^{-3}. To analyze and visualize the mapped reads, ngsplot was used (Shen et al., 2014). The motif analysis was performed using HOMER (Hypergeometric Optimization of Motif EnRichment) software (Heinz et al., 2010).

Exome analysis and direct sequencing

Genomic DNA of SCOS#2-A1, sarcoma iPSC#2-A1 and sarcoma-iPSC#2-A1-derived secondary sarcoma was extracted with PureLink® Genomic DNA Mini Kit (Invitrogen). Whole-exome capture was done with the SureSelect XT (Agilent Technologies). The exome libraries were then sequenced on a HiSeq2500 (Illumina). Raw sequencing reads were mapped to the mouse reference genome (mm10) using the Burrows-Wheeler Aligner (bwa-0.7.12) and were processed with SAMtools (samtools-1.2). Genome

Analysis Toolkit (GATK version: 3.5) was used to perform base recalibration and local realignment. SNVs and indels were called by the GATK HaplotypeCaller. We selected somatic variants by removing SNPs and indels reported in the mm10 (VCF file was downloaded from NCBI) and by removing the overlapping variants present in 129S1/Sv exome data (SRP007328). Remaining variants were annotated by SnpEff version 4.2 using RefGene GRCm38.82. To this end, we detected 15567, 16221 and 15338 variants including 577, 620 and 554 missense mutations in SCOS#2-A1, sarcoma iPSC#2-A1 and the secondary sarcoma, respectively. 405 missense mutations were overlapped in SCOS#2-A1, sarcoma iPSC#2-A1 and the secondary sarcoma. In order to extract unique mutations to this sarcoma model, the missense mutations were further compared with exome data of other tumor models (colon tumor and clear cell sarcoma model; submitted). A list of the unique mutations was shown in Table S2. For direct sequencing analysis, the PCR product containing the mutation candidate site was sequenced with the genetic analyzer ABI 3500xL (Applied Biosystems).

Supplemental References

Arioka, Y., Watanabe, A., Saito, K., and Yamada, Y. (2012). Activation-induced cytidine deaminase alters the subcellular localization of Tet family proteins. PLoS One *7*, e45031.

Beard, C., Hochedlinger, K., Plath, K., Wutz, A., and Jaenisch, R. (2006). Efficient method to generate single-copy transgenic mice by site-specific integration in embryonic stem cells. Genesis *44*, 23-28.

Feng, Y., Sassi, S., Shen, J.K., Yang, X., Gao, Y., Osaka, E., Zhang, J., Yang, S., Yang, C., Mankin, H.J.*, et al.* (2015). Targeting CDK11 in osteosarcoma cells using the CRISPR-Cas9 system. J Orthop Res *33*, 199-207.

Grilli, A., Sciandra, M., Terracciano, M., Picci, P., and Scotlandi, K. (2015). Integrated approaches to miRNAs target definition: time-series analysis in an osteosarcoma differentiative model. BMC Med Genomics *8*, 34.

Heinz, S., Benner, C., Spann, N., Bertolino, E., Lin, Y.C., Laslo, P., Cheng, J.X., Murre, C., Singh, H., and Glass, C.K. (2010). Simple combinations of lineage-determining transcription factors prime cis-regulatory elements required for macrophage and B cell identities. Mol Cell *38*, 576-589.

Kawano, M., Tanaka, K., Itonaga, I., Ikeda, S., Iwasaki, T., and Tsumura, H. (2015). microRNA-93 promotes cell proliferation via targeting of PTEN in Osteosarcoma cells. J Exp Clin Cancer Res *34*, 76.

Lu, J., Song, G., Tang, Q., Zou, C., Han, F., Zhao, Z., Yong, B., Yin, J., Xu, H., Xie, X.*, et al.* (2015). IRX1 hypomethylation promotes osteosarcoma metastasis via induction of CXCL14/NF-κB signaling. J Clin Invest *125*, 1839-1856.

Mackintosh, C., Ordóñez, J.L., García-Domínguez, D.J., Sevillano, V., Llombart-Bosch, A., Szuhai, K., Scotlandi, K., Alberghini, M., Sciot, R., Sinnaeve, F.*, et al.* (2012). 1q gain and CDT2 overexpression underlie an aggressive and highly proliferative form of Ewing sarcoma. Oncogene *31*, 1287-1298.

Miyagawa, Y., Okita, H., Nakaijima, H., Horiuchi, Y., Sato, B., Taguchi, T., Toyoda, M., Katagiri, Y.U., Fujimoto, J., Hata, J.*, et al.* (2008). Inducible expression of chimeric EWS/ETS proteins confers Ewing's family tumor-like phenotypes to human mesenchymal progenitor cells. Mol Cell Biol *28*, 2125-2137.

Ohta, S., Nishida, E., Yamanaka, S., and Yamamoto, T. (2013). Global splicing pattern reversion during somatic cell reprogramming. Cell Rep *5*, 357-366.

Shen, L., Shao, N., Liu, X., and Nestler, E. (2014). ngs.plot: Quick mining and visualization of next-generation sequencing data by integrating genomic databases. BMC Genomics *15*, 284.

Soleimani, M., and Nadri, S. (2009). A protocol for isolation and culture of mesenchymal stem cells from mouse bone marrow. Nat Protoc *4*, 102-106.

Takigami, I., Ohno, T., Kitade, Y., Hara, A., Nagano, A., Kawai, G., Saitou, M., Matsuhashi, A., Yamada, K., and Shimizu, K. (2011). Synthetic siRNA targeting the breakpoint of EWS/Fli-1 inhibits growth of

Ewing sarcoma xenografts in a mouse model. Int J Cancer *128*, 216-226.

Ullah, M., Sittinger, M., and Ringe, J. (2014). Transdifferentiation of adipogenically differentiated cells into osteogenically or chondrogenically differentiated cells: phenotype switching via dedifferentiation. Int J Biochem Cell Biol *46*, 124-137.

Varas, F., Stadtfeld, M., de Andres-Aguayo, L., Maherali, N., di Tullio, A., Pantano, L., Notredame, C., Hochedlinger, K., and Graf, T. (2009). Fibroblast-derived induced pluripotent stem cells show no common retroviral vector insertions. Stem Cells *27*, 300-306.

Zhang, Y., Liu, T., Meyer, C.A., Eeckhoute, J., Johnson, D.S., Bernstein, B.E., Nusbaum, C., Myers, R.M., Brown, M., Li, W.*, et al.* (2008). Model-based analysis of ChIP-Seq (MACS). Genome Biol *9*, R137.